Open Access

Journal of Energy and Power Technology

LIDSEN Publishing Inc.

Original Research

Experimental Vapor-Pressures and Derived Thermodynamic Properties of Geothermal Fluids from Baden-Baden Geothermal Field (Southeastern Germany)

Misirkhan A. Talybov [1], Lala A. Azizova [1], Ilmutdin M. Abdulagatov [2, 3, *]

1. Azerbaijan Technical University, Department of Thermal Engineering, Baku, Azerbaijan; E-Mails: misirkhantalibov@yahoo.com; akhmedova_la@yahoo.com
2. Geothermal Research Institute of the Russian Academy of Sciences, Makhachkala, Dagestan, Russia Federation
3. Dagestan State University, Makhachkala, Dagestan, Russian Federation; E-Mail: ilmutdina@gmail.com

* **Correspondence:** Ilmutdin M. Abdulagatov; E-Mail: ilmutdina@gmail.com

Academic Editor: Catalin Teodoríu

Special Issue: Advancement of Geothermal Technology for Sustainable Energy Production

Journal of Energy and Power Technology
2019, volume 1, issue 4
doi:10.21926/jept.1904006

Received: September 24, 2019
Accepted: December 12, 2019
Published: December 24, 2019

Abstract

***Background*:** In the present study, vapor-pressures of three geothermal fluids from Baden-Baden geothermal field (Kirchenstollen, Friedrichstollen, and Murquelle, southeastern region of Germany) were measured over the temperature range of 274–413 K. The combined expanded uncertainty of the temperature and vapor-pressure measurements at 95% confidence level with a coverage factor of k = 2 were estimated to be 0.01 K and 1–3 Pa at low and 10–30 Pa at high temperatures, respectively. The measured values of vapor-pressure were used to calculate other crucial derived thermodynamic properties of these geothermal fluid samples, such as enthalpy and entropy of vaporization and the heat capacity.

***Methods*:** The measurements were performed using two different methods and experimental apparatus: (1) absolute and differential static method which was used at low

temperatures ranging from 274.15 to 323.15 K; and (2) absolute static method which was used at elevated temperatures ranging from 323.15 to 413.15 K.

***Results*:** The data obtained from the measurements were utilized to formulate Antoine and Wagner-type vapor-pressure equations. The effects of various ion species on the vapor-pressure of the geothermal fluids were studied. In addition, the measured vapor-pressure values were utilized to develop Riedel's type correlation model for natural geothermal fluids in order to estimate the contributions of the various ion species to the total experimentally-observed values of vapor-pressure. It was observed that the anions were increasing the vapor-pressure, while the cations were decreasing it, with the rates (magnitudes) of these increases and decreases being different and strongly dependent on the chemical nature of the ion species involved. Using the measured vapor-pressure data, the other key thermodynamic properties, such as enthalpy and entropy of vaporization and the heat capacity) of the geothermal fluid samples were calculated.

***Conclusions*:** The measured vapor-pressure values of the geothermal fluids were higher than the pure water values (IAPWS standard data) by 5.5%–25.4% for Kirchenstollen, 3.0%–11.4% for Friedrichstollen, and 5.3%–14.8% for Murquelle, depending on the temperature. The largest deviations (up to 11%–25%) were observed at low temperatures (approximately 277 K), while at high temperatures, the deviations were within the range of 3.0% to 5.5%. This could be attributed to the effects of soluble gas in the geothermal fluids. The soluble gases were observed to be strongly affecting the measured vapor-pressure of the geothermal fluids. The experimentally observed vapor-pressure was the result of the competition between the opposite effects of the anion and cation contributions.

Keywords

Enthalpy of vaporization; geothermal fluids; heat capacity; thermodynamic properties; vapor-pressure; water

1. Introduction

Geothermal energy has great potential worldwide [1, 2]. In order to achieve the effective utilization of geothermal resources, precise thermodynamics and transport properties data are required for the initial resource estimates, production and reservoir engineering studies, and binary geothermal power cycle optimization. The energy characteristics of geothermal fluids would then be extracted directly from their thermodynamic property data [3]. Geothermal fluids are aqueous salt solutions that are heated by the natural heat flow from the earth (i.e., heated by natural hot rocks). High-temperature geothermal fluids with temperatures of approximately 120°C are generally used for electricity generation, while the low-temperature geothermal fluids (with temperatures below 60 °C) are used directly to supply thermal energy for applications such as agriculture, aquaculture, and space heating.

Accurate thermodynamic property data of the geothermal fluids at power plant operating conditions are important [4]. Using these data along with the chemical composition of the geothermal fluids enables proper power plant dimensioning, especially the size specification of the

heat exchanger, which is one of the main important components that determine the operational efficiency of the plant [5-7] and other geothermal energy utilization devices or the likelihood of scaling and/or corrosion development within the wells and the surface installations. The power plant design (energy production and equipment size) is considerably dependent on the thermo-physical properties of the geothermal fluid used. In order to utilize the geothermal resources as efficiently and economically as possible, and to ensure minimum disruption to the environment, modeling of the geothermal systems (multi-phase underground flows, phase transition processes in different reservoir zones, reservoir installations and wells, and geothermal engineering) is required, which in turn requires precise thermo-physical property data [8, 9]. Modeling of the geothermal system assists in determining its natural (prior to exploration) state and its behavior under exploration [5-7, 10-12]. The application of geothermal fluids for providing direct heat and for electricity generation requires reliable thermodynamic and transport property data which would determine the energy input of the plant, as was demonstrated in previous studies [13-15]. The total heat content (energy amount) of the geothermal fluid is dependent on its density, temperature, and heat capacity, as reported by Schröder et al. [10-12]. Imprecise knowledge of the geothermal water properties (isobaric heat capacity) leads to inaccurate knowledge of the geothermal water heat content, and in turn to incorrect knowledge of the heat input to geothermal power plants.

Geothermal fluids consist of complex mixtures of water, salts dissolved in a liquid phase, and dissolved gases [16]. Pure water is the main component of this mixture. Geothermal brines are mainly sodium chloride solutions. Sodium chloride (NaCl) typically constitutes 70%–80% of the total dissolved solids (TDS) in geothermal brines. Calcium is the other major cationic constituent of the geothermal brines. Chloride ion is the only major anionic constituent of these brines, while their second most important anionic ingredient is the bicarbonate ion. Due to the lack of thermodynamic properties of the data, in most cases, geothermal fluids were modeled as pure water [17] or as binary (H_2O+NaCl) [18] and ternary [19] aqueous salt solutions. Anderson et al. [20] developed a *PVT* model to predict the thermodynamic properties of a prototype geothermal fluid represented by the three-component H_2O+CO_2+NaC1 mixtures. The properties of these mixtures were used in numerical simulations developed for the natural geothermal fluids and as reference data for designing the power plant and its components [20, 21]. Seawater is the natural fluid that is the most similar to geothermal water because its main ionic constituents are similar to those in the geothermal fluids. The properties of seawater have been studied widely by several authors (see, for example, [22]). Besides the dissolved solids, geothermal fluids may contain considerable amounts of gases. The main representatives of non-condensed gases in the geothermal systems are CO_2, CH_4, H_2S, N_2, and H_2. The contents of salts and dissolved gases significantly alter the reservoir geothermal performance. Therefore, it is crucial to consider the effect of the constituent salts and dissolved gases on the thermo-physical properties of natural geothermal fluids [23].

The previous publications by our research group [24-27] report the experimental study of the density, speed of sound, heat capacity, and the viscosity of natural geothermal fluids obtained from various geothermal wells (Russia and Azerbaijan) and having different chemical compositions (varying with the locations). The present paper reports the continuation of the study on the thermodynamic and transport properties of these natural geothermal fluids. A detailed review of the previous studies on the properties of geothermal brines was provided in the recent

publications by our research group [24-26] (see also, Schrüder et al. [10-12]). Limited thermodynamic property data for natural geothermal brines have been published so far. Most of the reported data are for the geothermal brines having only binary or ternary aqueous salt solutions as their main components (basically for the synthetic geothermal brines). Schrüder et al. [10-12] proposed *in-situ* measurement techniques for the accurate measurement of the key physico-chemical properties of natural thermal water, such as isobaric heat capacity, density, and kinematic viscosity, at plant operating conditions, thereby avoiding the risk of changes in the water composition as a consequence of sample collection. Owing to the scarcity of data on the thermodynamic properties of geothermal fluids, an approach different from the one used previously for estimating these properties was adopted in certain studies [21, 28-36]. Wahl [37] proposed a linear function of salt concentration correlation for the density of geothermal brines. The simplest way to determine the thermodynamic properties of the geothermal fluids is the one based on pure water properties, because pure water is the dominant constituent, governs the properties (thermodynamic behavior) of the aqueous salt solutions and geothermal brines [38-42]. However, using direct experimental thermodynamic data of the particular natural geothermal fluid being studied allows minimization of the errors arising from empirical data prediction in geothermal brine models. Moreover, the brine composition may be altered during production. Therefore, direct measurements of natural geothermal brines from various regions (wells) throughout the world containing various concentrations of dissolved electrolytes are required. This would allow the generalization of the properties of various geothermal fluids from various geothermal fields (locations) containing various solutes and would assist in developing prediction models for geothermal brines with any chemical composition. Unfortunately, the currently available theoretical models are often unable to describe the real systems that are in practice. For instance, accurate prediction of the thermodynamic and transport properties of complex multi-component ionic aqueous solutions such as geothermal fluids is extremely difficult due to their complexity. In the microscopic point of view, the effect of individual ionic contributions to the properties of the aqueous solution is dependent on the structure of the ions (shape, size, ionic environment, polarization orientation, ion mobility, *etc*.). Even for the binary aqueous salt solutions, it is quite difficult to accurately estimate the effect of ions on their properties. It is almost impossible to accurately estimate the effect of all the dissolved salts on the properties due to the extremely complex interactions among the salt ions, dissolved gases, and the water molecules and the ion-ion interactions in the multi-component aqueous solutions. Therefore, accurate thermodynamic data for natural geothermal fluids are of interest to the scientific researchers for the study of the fundamental physico-chemical basis of the theory of multi-ionic interactions on the microscopic level. Models with better predictive abilities may be developed on the basis of reliable direct experimental information on the thermodynamic and transport properties of natural geothermal brines. However, experimental study of the thermodynamic properties of each geothermal fluid is a formidable task, and therefore, theoretical or semi-empirical models that would be able to predict the thermodynamic properties of complex geothermal brines would be useful. In order to quantitatively describe the thermodynamic and transport properties of geothermal fluids as a function of T, P, and x, a thermodynamic model (equation of state) or a reference correlation model for the transport properties would be required. In addition, direct measurements of the thermo-physical properties of natural

geothermal brines with complex compositions are required to confirm the applicability and accuracy of the mixing rules.

2. Materials and Methods

2.1 Characteristics of Geothermal Field Location and Wells

The three geothermal fluid samples used in the present study were collected from three geothermal hot wells in Baden-Baden geothermal field, Germany [Kirchenstollen (48°45'47.60" N, 8°14'29.17" E), Friedrichstollen (48°45'49.40" N, 8°14'31.35" E), and Murquelle (48°45'48.62" N, 8°14'33.66" E)]. The geothermal field is located in the eastern part of the Rhine (Baden-Baden) trough. The area map (locations of the hot wells) with the potential for hydrogeothermal exploitation in Germany may be obtained from certain previous reports [43, 44]. The depths of the wells from which the samples were obtained ranged from 1200 to 1800m. The well-head temperatures T_{wh} were within the range of 64.5–69 °C. The debit was approximately 800,000 L/day (9.26 L/sec). The geothermal gradient in this region varied from 3 to 10 °C/100 m.

The most important geological settings for geothermal energy in Germany arethe deep Mesozoic sediments, which may be located in the North German Basin, the Upper Rhine Graben, and the South German Molasse Basin [43]. Several projects are under development in the Upper Rhine Graben, which is one of the regions with hydrogeothermal potential. Above-average geothermal gradients render this region interesting for the development of electricity projects [45]. The new 5 MWe ORC plant of Insheim in the Upper Rhine Graben began producing geothermal electricity in November 2012,and heat extraction is planned in the further development of the project [45]. Most of the geothermal plants are located in the Molasse Basin in southern Germany, along the Upper Rhine Graben. The main objective of the present study was the accurate measurement of the vapor-pressure of three natural geothermal fluids obtained from the Baden-Baden geothermal field (Kirchenstollen, Friedrichstollen, and Murquelle, Germany) as a function of temperature in the range of 274.15–413.15 K. In the present work, a detailed experimental study of the effects of dissolved salts (salinity, and therefore, the effect of location), nature of the chemical composition, and soluble gases on the temperature behavior of vapor-pressure of the geothermal brine samples collected from the Baden-Baden geothermal field was performed. The present work provides accurate vapor-pressure and a few derived key thermodynamic properties data (enthalpy and entropy of vaporization and the heat capacity) for the three natural geothermal brines with different mineralogical compositions, collected from the Kirchenstollen, Friedrichstollen, and Murquelle hot wells in Germany. The study area (Baden-Baden) has great geothermal potentials, holds the highest position among the places for balneological treatment and society events, and is one of the most prestigious and historic thermal spas in Germany. The existence of these hot springs has been associated with the deep faults located at the eastern end of the Upper Rhine Graben. The location of the springs was in use in the middle of 19th-century post-1868, and a system of tunnels had been constructed to catch the springs and to increase the production and temperature. The system consisted of two main tunnel areas, one just below the castle with “Friedrichstollen” as the main tunnel, and the other close to the marketplace with “Kirchenstollen” and “Rosenstollen”. A new, large bathing facility, the “Friedrichsbad”, was built later. The geothermal gradient in the second of the deep holes was measured to be 5.1 °C/100 m. This appeared promising for the use of geothermal energy if either water could be found or the

technologies from the Hot-Dry-Rock development could be used. Currently, the activities in Baden-Baden are dominated by two major bathing facilities. One of these two facilities is the traditional Friedrichsbad, which has been serving to provide relaxation and healing for greater than a century. Friedrichsbad receives its supply of thermal water from the traditional hot springs as well as from the two wells drilled in the 1960s. The thermal water is also delivered to three public drinking fountains and to several private users (such as hotels for hot bathing, hospitals for healing purposes, etc.). The annual consumption of thermal water from Friedrichsbad is 83,621 m^3/year. Geothermal district heating is accomplished with two or more geothermal wells, with at least one serving as a production well and one serving as an injection well. Re-injection of the cooled geothermal fluids is necessary to maintain the pressure in the reservoir and to avoid the contamination of surface waters or the shallow aquifers with high salt loads or toxic fluid constituents. Several hot springs supply thermal water to the spa facilities, with temperatures ranging from 52 to 67 °C and mineralization within the range of 2680–3522 mg/kg. The total thermal water production in Baden-Baden is 9.4 L/s. The thermal water has an energy content of 2 MW, although complete energy use has not been achieved so far [4].

2.2 Sample Description

Thermodynamic properties of natural geothermal fluids are affected strongly by their chemical composition (concentration and the type of salt and gas contents, as stated earlier). Geothermal fluid is a brine solution formed as a result of the natural movement of water through the crust of the Earth. The brine compositions vary from well to well, depending on the depth of the production and the temperatures of the different parts of the reservoir [46] which lead to the precipitation of certain components (phase-equilibrium behavior of brine at different pressures and temperatures). Therefore, the geothermal fluids collected from different wells have different chemical compositions, and their properties also vary. Studies conducted on the composition of dissolved ions in the geothermal fluids [24-26] have indicated considerable variations when moving from one area to another.

The chemical compositions of the geothermal fluid samples collected from the Kirchenstollen, Friedrichstollen, and Murquelle hot wells of the Baden-Baden (Germany) geothermal field are listed in Table 1. An IRIS Intrepid II Optical Emission Spectrometer and ion chromatography techniques were utilized for the quantitative determination of the elemental composition (cations and anions) of the geothermal brine samples. The accuracy ranged between 0.2% and 1.0%. The elements were ionized in the argon plasma flame and were analyzed using a high-resolution mass spectrometer. As observable from Table 1, the total mineralization values for the geothermal fluid samples from the Kirchenstollen, Friedrichstollen, and Murquelle wells were 2.74 g/L, 2.60 g/L, and 2.75 g/L, respectively, i.e., all the values were almost equal. The main chemical composition distributions for the hot-wells obtained on the basis of the data in Table 1 are presented in Table 2. As it may be noted from Table 2, the main components of the geothermal fluid samples were: chloride (52.9%to 55.9%), sodium (26.1% to 28.7%), sulfate (6.7% to6.8%), calcium (3.9%to 4.4%), potassium (2.2%to 2.4%), and Si and S (1.9% to 2.1%). Therefore, the major mineral components in the studied geothermal fluid samples were Cl^-, Na^+, SO_4^{-2}, Ca^{+2}, K^+, Si^+, and S^+. Salinity was derived mainly from Na^+, K^+, Ca^{+2}, Si^+, and S^+, and from SO_4^{-2} and Cl^- ions, all of which together comprised approximately 71% to 73% of all the compounds in the fluid solution. All the samples

exhibited similar concentrations of Na^{+}, Ca^{+2}, K^{+}, Si^{+}, S^{+}, SO_4^{-2}, and Cl^{-}, indicating relatively homogenous compositions at that depth. The pH-values of the samples measured on the surface immediately after pressure release varied between 6.43 and 7.47. The composition of a particular well was observed to vary as a function of the total production time, the rate of flow, and the nature of the underlying sediments. Table 3 compares the main chemical compositions of the geothermal fluid sample from hot-well Friedrichstollen as determined in the present study with the data reported by Sanner [4] in 2000. As observable from Table 3, there was a slight increase in the sodium (by 14%), potassium (19%), lithium (27%), calcium (12.5%), chloride (4.6%), and nitrate (46%) contents, and a decrease in the magnesium (by 90%) and sulfate (14.7%) contents. The main gas contents [together constituting approximately 90% to 95% of the gas content] in the samples were nitrogen, carbon dioxide, methane, hydrogen, argon, helium, and oxygen. The carbon dioxide content in the samples was approximately 132 mg/L (or approximately 5%). Prior to the measurements, the geothermal brine samples were filtered for the removal of suspended solids using filters of 2-micron pore size.

Table 1 Chemical compositions of the geothermal brines.

Species	**Kirchenstollen**	**Friedrichstollen**	**Murquelle**
	(*mg/l*)	(*mg/l*)	(*mg/l*)
		Cations	
Al1862	<0.01	0.02	<0.01
As1890	0.12	0.13	0.12
B2089	1.34	1.31	1.26
Ba2304	0.13	0.15	0.12
Ca3181	**107**	**115**	**116**
Cd2288	<0.01	<0.01	<0.01
Co2286	<0.01	<0.01	<0.01
Cr2055	<0.01	<0.01	<0.01
Cu3247	<0.01	<0.01	<0.01
Fe2599	0.03	0.02	<0.01
Hg1849	<0.02	<0.02	<0.02
K7664	**61.8**	**63.0**	**60.7**
Li6707	7.23	7.11	6.81
Mg2790	3.31	3.93	3.81
Mn2939	0.26	0.38	0.26
Mo2045	<0.01	<0.01	<0.01
Na8183	**716**	**745**	**728**
Ni2316	<0.01	<0.01	<0.01

P2136	<0.01	<0.01	<0.01
Pb2203	<0.01	<0.01	<0.01
S1820	**51.90**	**52.10**	**52.70**
Sb2175	<0.02	<0.02	<0.02
Se1960	<0.02	<0.02	<0.02
Si2124	**55.00**	**55.40**	**52.80**
Sn1899	<0.01	<0.01	<0.01
Ti3349	<0.01	<0.01	<0.01
Tl1908	<0.01	<0.01	<0.01
V2924	<0.01	<0.01	<0.01
	Anions		
Chloride	**1548.0**	**1375.0**	**1537.0**
Nitrate	3.3	3.7	4.5
Sulfate	**183.7**	**177.9**	**183.9**
Total dissolved salt	**2739.4**	**2600.33**	**2748.18**

Table 2 Distribution of main chemical composition for the geothermal fluid samples.

Hot-well	**Kirchenstollen**	**Friedrichstollen**	**Murquelle**
Sulfate	6.7 %	6.8 %	6.7 %
Chloride	56.5%	52.9 %	55.9 %
Sodium	26.1 %	28.7 %	26.5 %
Sulfur	1.9 %	2.0 %	2.1 %
Silicon	2.0 %	2.1%	1.9%
Calcium	3.9 %	4.4 %	4.2 %
Potassium	2.3 %	2.4 %	2.2 %

Table 3 Comparison of the main chemical composition for geothermal fluid samples for hot-well Friedrichstollen.

Species	Friedrichstollen (this work)	Friedrichstollen (Sanner [4])
	Cations (mg/*l*)	
Sodium	745.00	850.66
Potassium	63.00	75.05
Lithium	7.11	9.03
Calcium	115.00	129.35
Magnesium	3.93	2.07
	Anions (mg/*l*)	
Chloride	1375.00	1437.60
Nitrate	3.7	5.4
Sulfate	177.9	155.1

2.3 Vapor-Pressure Measurements

As stated earlier in the Introduction section, vapor-pressure is a property of natural water that is highly sensitive to salt and gas concentrations. In order to achieve an accurate estimation of salinity based on its relationship with vapor-pressure, which is comparable to the accuracy achieved in the direct measurement of salinity, a vapor-pressure uncertainty of <3 Pa at low temperature and <30 Pa at high temperature is required. In this context, substitution measurement involving two methods has been proposed in the present study. The measurements were performed using two different experimental techniques and apparatus: (1) absolute and differential static method used at low temperatures ranging from 274.15 to 323.15 K; and (2) the absolute static method used at elevated temperatures ranging from 323.15 to 413.15 K. The vapor-pressure measurements of the geothermal fluid samples collected from the Baden-Baden geothermal field (Germany) for the present study were performed at the Department of Technical Thermodynamics, Rostock University.

The main part of the experimental apparatus (Figure 1) for the vapor-pressure measurements at low temperatures (ranging from 274.15 to 323.15 K) consisted of glass cells–3,4, and 27. These glass cells comprised inner and outer volumes in which the distilled water supplied from thermostat–21 (Lauda Gold R–415, Germany) flowed. The temperature inside these measurement cells was achieved and stabilized by using a thermostat–21 with an uncertainty of 0.01 K. The temperature was measured using PRT–100–6 and 35, with an uncertainty of 0.01 K. The volume of each glass cell was approximately 80 cm^3. In case of solutions with low concentration, for which the vapor-pressure was quite close to the vapor pressure of the solvent (i.e. if the vapor-pressure difference was approximately 10 to 30 Pa, within the uncertainty range of the static cell), the measurements were performed in the differential part–3 and 4 of the experimental apparatus. In this part, both the cells were immersed in the same water reservoir. The temperature in the reservoir was measured using PT–100–6 (Figure 1), with an uncertainty of 0.01 K. The vapor-pressure values in the measurement cells were measured using high-precision pressure meters–

10,MKS Baratron type 616A (USA) in the differential part of the apparatus with an uncertainty of 1–3 Pa and MKS Baratron type 615A-23 (USA) in the static part with an uncertainty of 10–30 Pa. These measurements were performed at the temperature of 333.15 K within the reservoirs-11 which were thermostated to maintain a constant temperature. Water was supplied to the reservoir through a thermostat Haaki (Germany). The derived results were transmitted to the pressure signal indicators–13 and 14 (Figure 1) through the adapters–12 and 15, and then directly to the computer–34 using the LabVIEW software. The measured temperature values were also transmitted to the same computer–34. The computer-controlled the stabilization of the vapor-pressure at a given temperature, and after measuring the pressure, it changed the temperature of the experiment to the next one at a given interval to the maximum value. When the maximum temperature of the experiment was reached, the computer changed the temperature in the opposite direction, and the vapor-pressure was then measured to the minimum temperature. Therefore, a repetition of the experimental points occurred. The repeatability could also be established in advance using a computer software system. Prior to the commencement of the measurements, the measurement cells were washed thoroughly with water and acetone, followed by being vacuumed using a vacuum system–31 to 33 (Figure 1). The magnets–2 and 36 located in the measurement cells were kept rotating inside the cells using magnetic stirrers–1 and 28, which assisted in reaching the equilibrium condition (stabilization of the liquid–vapor system). Since the measurement cells and the pressure meter MKS Baratron were located at a distance of 40 cm from each other, in order to connect them, a special design had to be used. Therefore, special adapters «glass–metal» from MDC vacuum Limited (England) were welded to the glass measurement cells, and the special nozzles from VAT Deutschland GmbH were welded to the metallic part of the adapters «glass–metal». In-between these nozzles, sealing discs with a rubber gasket were mounted. The second nozzle was connected with the pressure meter using a capillary tube. This design lowered the uncertainty in the vapor-pressure measurements. However, it could not completely eradicate all the possible sources of uncertainty. The design could be evaluated for accuracy of measurement by using the standard fluids, such as water, alcohol, or hydrocarbons, the vapor-pressures for which are well-known (REFPROP/NIST [47]). In order to avoid loses, the portion between the glass measurement cells and the pressure meter MKS Baratron was heated using electrical (8 and 25) and water (9 and 24) heaters. The accuracy and reliability of the measured vapor pressure data for the studied geothermal fluids, as well as the correct operation of the experimental apparatus, were verified by measuring the vapor-pressures of the well-studied standard fluids, such as pure water, methanol, ethanol, acetone, etc., for which reliable reference data are available (REFPROP, NIST [47]).

Approximately haft of the measurement cell was filled with the sample to be studied. The special flask connected to a metal tip–7, 20, and 38–was used to fill the cell. After filling the measurement cells with the sample to be studied, part of the sample evaporated to form the vapor phase, creating saturated vapor pressure above the liquid phase. After a little while, when the system in the measurement cell approached the equilibrium condition, the vapor-pressure measurement was begun. Since geothermal fluids consist of complex mixtures of water, salts dissolved in the liquid phase, and dissolved gases, it is crucial to consider the effects of salts and dissolved gases on the measured vapor-pressure of natural geothermal fluids. Therefore, the experiments conducted with the geothermal fluids in the present study actually measured the vapor-pressure of the aqueous salt solutions with a vapor phase consisting of a mixture of water

vapor and soluble gases. Therefore, the saturated vapor pressure of the geothermal fluids was the sum total of the saturated vapor-pressures of water and soluble gases. The soluble gases exerted a strong influence on the measured vapor-pressure of geothermal fluids.

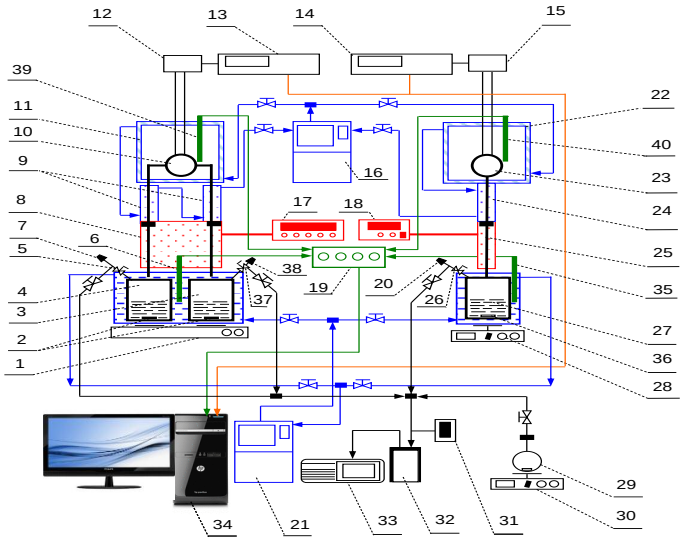

Figure 1 Schematic diagram of the experimental apparatus for vapor-pressure measurement at low temperatures (from 274.15 to 323.15 K). 1, 28, and 30-magnetic stirrers; 2 and 36-magnets; 3-measuring cell for differential method of vapor-pressure measurements for pure water; 4-measuring cell for differential method of vapor-pressure measurements for the sample; 5 and 37-valves for closing of the measuring cell of the differential and static-26 methods for the vapor-pressure measurement of the sample; 6, 35, 39, 40-PRT with a four-channel input module for receiving and accumulating the temperature data (Омега PT–104A–19); 7, 20, and 38-connections for sample filling; 8-electrical heating of the cell connections with the pressure meters MKS Baratron 616Aand 25-MKS Baratron615 A; 9-water heating cell connections with pressure gauges MKS Baratron 616A and 24-MKS Baratron 615 A; 10-pressure gauge MKS Baratron 616Afor differential method and 23-MKS Baratron 615 Astatic method; 11-reservoir for maintaining a constant temperature for the pressure meter in the differential and 22-in static methods; 12-connector of the pressure signal with pressure indicator for differential and 15-static methods; 13-pressure signal indicator for differential and 14-static methods; 16-thermostat HAAKE F5; 17-electric heater control systems for differential and 18-static methods; 21-thermostat Lauda Gold R–415; 27-measuring cell for static method; 29-flask with a sample under study for filling; 31-vacuum indicator TTR100; 32-liquid nitrogen trap; 33-vacuum pump; 34- PC for control.

The above-described experimental apparatus (glass cells) cannot be used for the measurements of vapor-pressure at high temperatures (above atmospheric pressure). Therefore, a novel apparatus design was developed for the vapor-pressure measurements at temperatures ranging from 323.15 to 413.15 K (Figure 2). This newly designed experimental apparatus consisted of metallic cells prepared from stainless steel V4A (Germany). The inner volume of each cell was approximately 140 cm^3, which included the volumes of the cell and the connecting tubes as well as

haft the volume of the valve–10 (without the volume of PT–2 and 3 inside the cell). The measurement cell located inside the reservoir–12 was filled with silicon oil (KORASILON oil M50, Kurt Obermeier Gmb H&Co. KG, Germany). The desired temperature in the measurement cell was achieved using a thermostat–1 (LAUDA ECO RE 415 G, Germany) with an uncertainty of 0.01 K. The temperature inside the cell was measured using two platinum resistance thermometers–2 and 3 (PRT–100, 1/10 DIN Class B, Temperatur Messelemente Hettstedt GmbH, Germany). PRT–100 was connected to a four-channel input module for receiving and accumulating the temperature data–5 (Омега PT–104A, Omega Engineering, Inc., USA). One of the two thermometers was connected to the thermostat for direct transmission of information. Using this thermometer, the thermostat created the measured temperature directly inside the measurement cell and not in the thermostat itself. This was crucialas this method allowed creating any desired temperature with high accuracy directly inside the measurement area. The second thermometer (PRT–100) transmitted the measured temperature to the computer. The vapor-pressure was measured using the pressure meter–4 (SERIE 35 × HTC, Omega Gmb H&Co., Germany) with an uncertainty of 2,000 Pa. After each time interval, which was predetermined (usually 1 min), the vapor-pressure of a sample was measured and transmitted to a computer. Stationary operation with a constant temperature was achieved in approximately 50–70 min. This method and the described experimental apparatus have already been used successfully for the one-phase *PVT* and two-phase vapor-pressure measurements of a natural water sample from the Azerbaijan geothermal field in a previous study conducted by our research group [26].

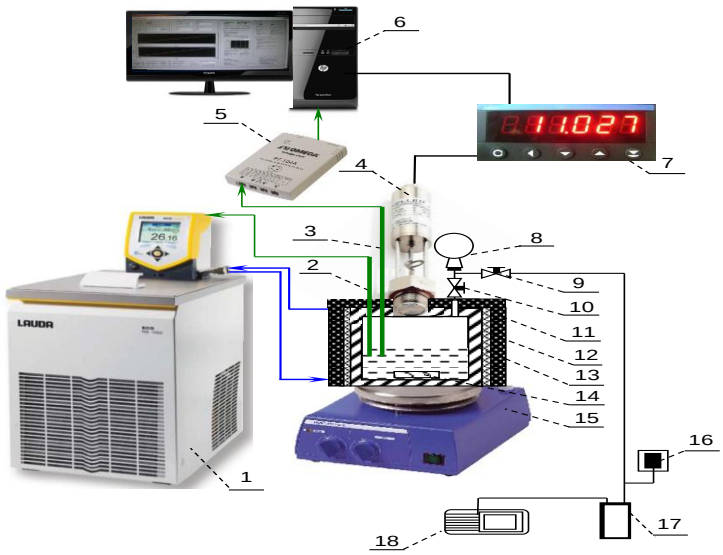

Figure 2 Schematic diagram of the experimental apparatus for vapor-pressure measurement at elevated temperatures (from 323.15 to 413.15 K). 1-thermostate LAUDA ECO RE 415 G; 2 and 3 PRT; 4-pressure measurement unit (pressure transducer) SERIE 35 × HTC; 5-four-channel input module for receiving and accumulating temperature data Омега PT–104A; 6-PC control; 7-pressure indicator; 8-flask with a sample under study for filling; 9 and 10-valves; 11-measuring cell insulation; 12-reservoir for maintaining a constant temperature in the measuring cell; 13-measuring cell; 14-magnet; 15-magnetic stirrer; 16-vacuum indicator TTR100; 17-liquid nitrogen trap; 18-vacuum pump.

3. Results and Discussion

In the present study, vapor-pressure values of the three geothermal fluid samples collected from Baden-Baden geothermal field (Kirchenstollen, Friedrichstollen, and Murquelle, Germany) were determined as a function of temperature over the temperature range of 274–413 K. The measured vapor-pressures for the geothermal fluid samples are listed in Table 4 and depicted as a function of temperature and ion species concentration in Figure 3 and Figure 4, respectively. Figure 3 also includes the vapor-pressures for pure water calculated using the IAPWS formulation (Wagner and Pruß [48]). As observable from Figure 3, the vapor-pressure data for the geothermal fluid samples exhibited the temperature behavior (*P*-*T*) similar to pure water (Wagner and Pruß [48]). However, the measured vapor-pressure values for the geothermal fluids were higher by a factor of 3%–25% compared to those for pure water, depending on the temperature of measurement. The differences (percentage deviations) between the measured vapor-pressure values for the geothermal fluids obtained in the present study and the pure water values published previously (Wagner and Pruß [48]), as a function of temperature, are presented in Figure 5. As visible in the figure, the deviations varied with temperature within the range of 5.5%–25.4% for Kirchenstollen, 3.0%–11.4% for Friedrichstollen, and 5.3%–14.8% for Murquelle, all of which were considerably higher than the corresponding experimental uncertainties of 0.02% to 0.08%. The maximum deviations (in the range of 11%–25%) were observed at low temperatures (approximately 277 K), while at high temperatures, the deviations were within the range of 3.0%–5.5%. As may be noted from Figure 3, the measured values of vapor-pressure were higher than those in the reference data for pure water, although, for most of the aqueous salt solutions, vapor-pressure was lower than that of the pure water (see Figure 3 for H_2O+NaCl solution [49-51]). This could be attributed to the effect of soluble gases present in the geothermal fluids. It is well-known that soluble gases strongly affect the measured vapor-pressure of the geothermal fluids [20, 21] (see below). Large differences in the range of 2.6%–18.7% were observed between the vapor-pressure data for the Kirchenstollen and the Friedrichstollen samples, while the data for the Kirchenstollen sample deviated from those for the Murquelle sample by 0.1%–14%. The relatively low difference in the range of 2.5%–3.9% was observed between the Friedrichstollen and the Murquelle geothermal fluid samples. Vapor-pressure is a property that exhibits relatively higher sensitivity to salt and gas concentrations compared to the other thermodynamic properties such as density, heat capacity, and speed of sound (see, for example, Abdulagatov et al. [24-26]). Therefore, the vapor-pressure data measured at standard conditions may be utilized for the determination of the salt content and its variations in a geothermal fluid, i.e., accurate measurements of the vapor-pressure–salinity relationship may be applied in the estimation of salt concentration. Measurement of thermophysical properties has been frequently used to evaluate the quality of products; in particular, properties such as density, vapor-pressure, and viscosity are highly sensitive to the composition of a product. The quality of natural water may be determined through its physical, chemical, and microbiological properties. It is important to establish the quality of the natural water sources that are to be used for different purposes, in terms of specific water-quality parameters that would affect the possible use of water the most. Vapor pressure is a crucial and highly sensitive property of the liquids (in particular, natural water) for their quality analyses (for example, composition changes), i.e., it is the most sensitive indicator of any changes in the quality of natural water. The difference between the vapor-pressure of distilled pure water

and natural water is of the order of just a small magnitude depending on composition (see, for example [27]). The more accurate the vapor-pressure measurement, the more accurate is the determination of salinity (by means of the vapor-pressure–salinity relationship).

Table 4 Measured values of temperature (*T* / K) and vapor-pressure (*P* / kPa) of the geothermal fluids from Baden-Baden Geothermal Filed (Germany).

***T*/K**	***P*/kPa**	***T* / K**	***P*/kPa**	***T* / K**	***P*/kPa**
Kirchenstollen		**Friedrichstollen**		**Murquelle**	
274.17	0.882	274.17	0.743	274.18	0.773
278.16	1.160	278.15	0.984	278.15	1.021
282.73	1.571	283.47	1.410	283.36	1.452
292.32	2.863	298.76	3.653	292.20	2.552
303.16	5.348	308.38	6.284	301.47	4.423
313.20	9.123	318.17	10.499	313.15	8.379
322.98	14.792	323.32	13.556	323.19	13.908
333.16	23.632	333.17	21.549	333.17	22.228
343.17	36.315	343.16	33.427	343.18	34.478
353.16	54.238	353.15	50.404	353.19	51.984
363.10	78.858	363.10	73.970	363.10	76.107
373.10	112.328	373.12	106.324	373.11	109.283
383.15	156.961	383.11	149.458	383.13	153.665
393.18	215.024	393.14	206.284	393.15	211.895
403.16	289.029	403.10	279.164	403.14	286.758
413.11	382.021	413.13	372.297	413.13	381.781

Standard uncertainties *u* are: *u(T)*=0.005 K; *u(P)*=0.01 % at low temperatures (<323 K) and *u(P)*=0.04 % at high temperatures (>323 K) (level of confidence=95 %).

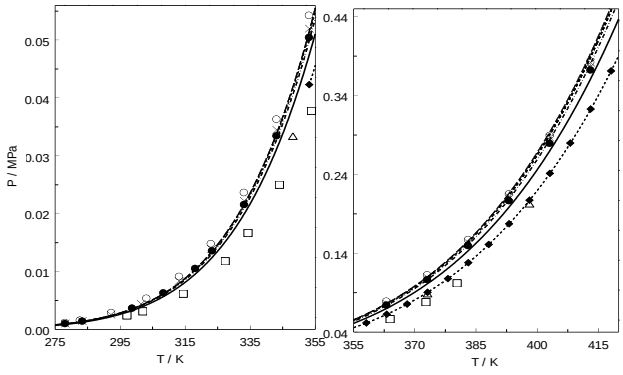

Figure 3 Detailed view of the temperature dependence of the measured values of vapor-pressure of geothermal fluids from Baden-Baden Geothermal Filed together with pure water values (solid lines) (IAPWS fundamental, Wagner &Pruß [48]) in distinct temperature ranges. ○-Kirchenstollen; ●-Friedrichstollen; ×-Murquelle; ♦-H_2O+NaCl [49]; △- H_2O+NaCl [50]; □- H_2O+NaCl [51]. The dashed line is calculated from correlation for H_2O+NaCl + CO_2 mixture [20]; Dashed-dotted line is the values of vapor-pressure calculated from correlation for H_2O+N_2 mixture [20].

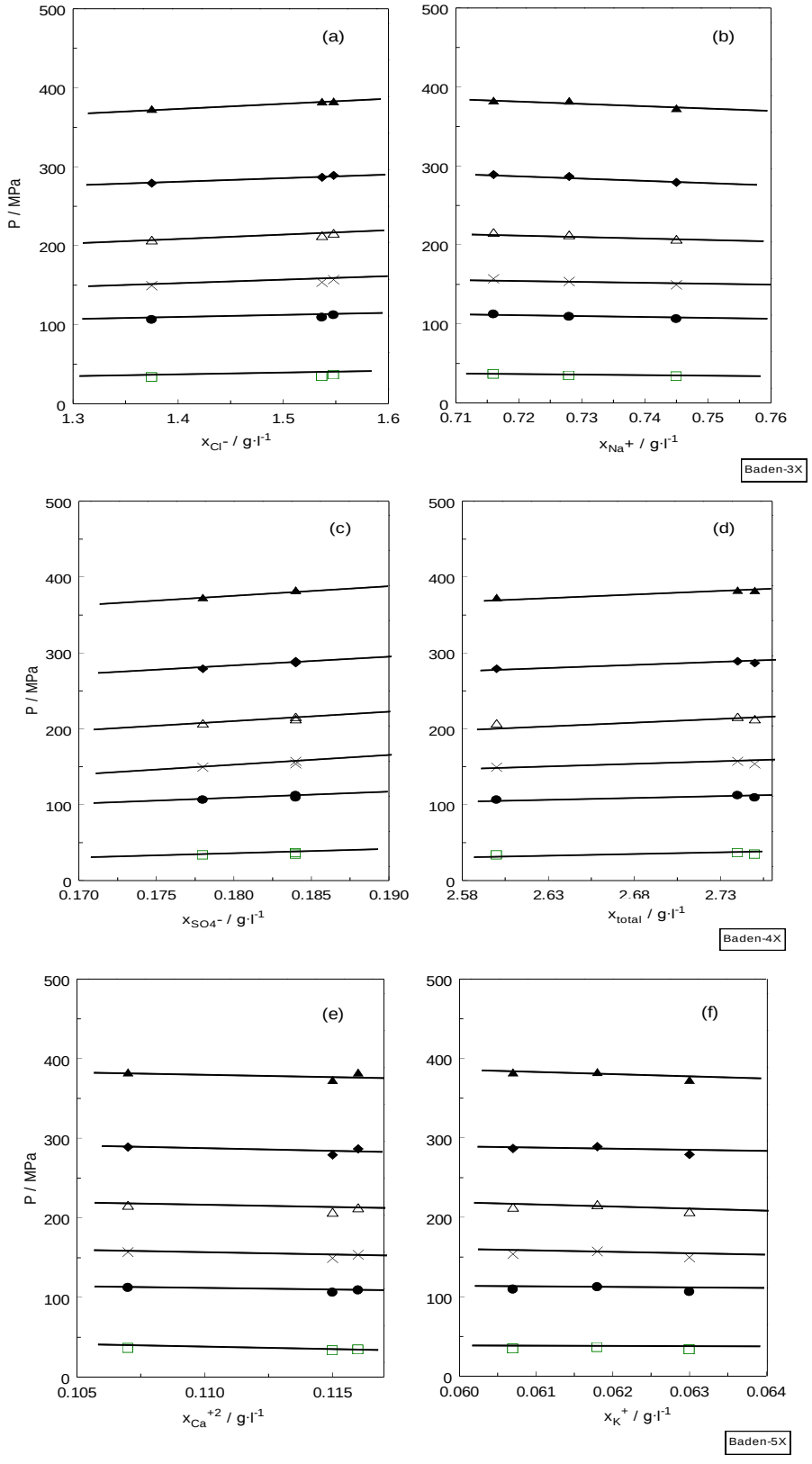

Figure 4 Effect of various ion species on the vapor-pressure of geothermal fluids along the different isotherms. (a)- Cl^-; (b)- Na^+; (c)- SO_4^{-2}; (d)- total ions concentration; (e)- Ca^{+2}; (f)- K^+;□–343 K; ●–373 K; ×–383 K; △–393 K; ♦–403 K; ▲–413 K.

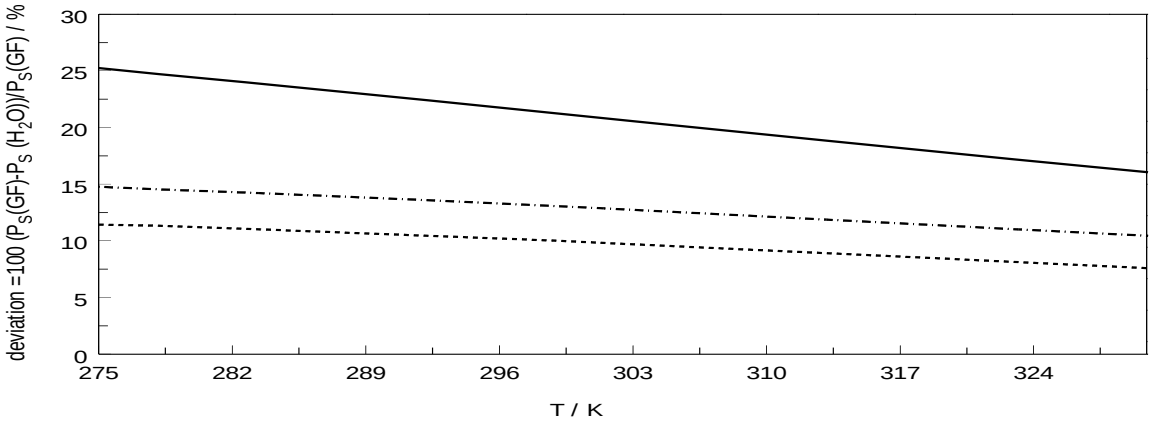

Figure 5 Percentage deviations between the present measured vapor-pressures for geothermal fluids and pure water (IAPWS formulation [48]). Solid line is Kirchenstollen; Dashed line is Friedrichstollen; and Dashed-dotted line is Murquelle.

The pressure from the dissolved gasses escaping the liquid phase adds to the total vapor pressure of a solution. If the water contains a huge amount of dissolved gasses, such as CO_2, then the vapor pressure of the solution is greater than that of the pure water. The individual vapor pressures of all ingredients of the solution contribute to the total vapor pressure of the solution. Vapor pressure is a property of a liquid and is dependent on two factors: one is temperature and the other is the presence of solutes or other liquids that interact significantly with the liquid. In the case of geothermal fluids, the liquid phase is formed by water and a group of non-volatile solutes and certain dissolved gases such as CO_2 or others (see above), which interact strongly with the water molecules. In regard to a solution with one liquid and several non-volatile solutes (salts, for example), Raoult's law states that the vapor pressure of an impure solution is always lower than that of a pure solvent. Therefore, an aqueous salt solution has a vapor pressure value lower than that of pure water. Figure 3 also presents the values of experimental vapor-pressures for the ternary mixture of H_2O+CO_2+NaCl which were reported by Anderson et al. [20] (see also, [21]). It may be noted that the vapor-pressure of the ternary aqueous system of H_2O+CO_2+NaCl containing dissolved $CO_2$was considerably higher than those of pure water and the aqueous solution of H_2O+NaCl. In general, for the vapor-pressure measurement, geothermal fluid may be modeled as a few basic primary aqueous salt solutions (depending on the basic component of the geothermal brine) and certain dissolved gases, using appropriate mixing rules. It is apparent that the difference in the vapor-pressure of various geothermal fluid samples was the result of the differences in their composition, i.e., it was the effect of the concentrations of constituent salts and dissolved gases. However, in certain cases, even the geothermal fluids with the same values of total mineralization (salinity) exhibited sufficient difference in their vapor-pressure values and other thermodynamic properties. This implied that the type of constituent ions also affected their properties to a considerable extent, i.e., the thermophysical characteristics of the geothermal fluids are dependent on, in addition to the total salt content (total mineralization), the chemical nature of the constituent ion species. For instance, the total mineralization values for the samples collected from Kirchenstollen and Murquelle were almost equal: 2.74 g/L and 2.75 g/L, respectively; however, their vapor-pressure values differed by 0.1% to 14%. This was probably caused by the differences in their sulfur, silicon, calcium, and/or dissolved gas contents. The

mechanism through which the chemical nature of the ion species and soluble gases in the geothermal fluids affect their total measured properties remains unclear. Figure 4 illustrates the effects of various ion species on the vapor pressure of the geothermal fluid samples along various isotherms. As may be noted in the figure, different types of ion species affected the vapor pressure differently. For instance, Cl^- and Na^+ ions exerted opposite effects on the vapor-pressure, i.e., Cl^- was observed to be increasing the vapor pressure, while Na^+ was decreasing it. In general, as inferred from Figure 4, anions were increasing, while the cations were decreasing the vapor-pressure. Certainly, the rate, $\left(\partial P_S / \partial c_i\right)_{\mathrm{T,C_{j\neq i}}}$, of these increases or decreases caused by the ion species was different and was strongly dependent on the chemical nature of the ion species. For instance, the same concentrations of Cl^- and Na^+ ions exerted different effects on the measured vapor-pressure; at a temperature of 413 K, the value of $\left(\partial P_S / \partial c_i\right)_{\mathrm{T,C_{j\neq i}}}$ for Cl^- ions was 57.2 kPa/(g/L), while that for the Na^+ ions was −350.02 kPa/(g/L). Overall, the resultant effect of the various types of ion species was dependent strongly on the multi-ionic interactions between the different types of ion species and the water molecules. The experimentally determined vapor-pressure value was the result of the competition between the opposite effects of anion and cation contributions. As stated earlier, from the microscopic point of view, the effect of individual ion contributions to the vapor-pressure of a geothermal fluid was dependent on their structure (shape, size, ions environment, polarization orientation, ion mobility, etc.). Owing to the complexity of the multi-ionic interactions among the various types of ion species in the geothermal fluids, it is impossible to theoretically predict the temperature and concentration dependence of vapor-pressure and the other properties. Therefore, this evaluation is empirical and based solely on the measured data.

In the present study, the vapor-pressure data for the geothermal fluid samples were fitted to the following correlation equation:

$$P_S\left(T, c_i\right) = P_{\mathrm{SH_20}}\left(T\right)\left(1 + \sum_{i=1}^{n} a_i c_i\right) \tag{2}$$

where $P_{\mathrm{SH_20}}(T)$ is the vapor-pressure of pure water (IAPWS formulation, Wagner and Pruß [48]), at temperature *T*; *n* is the number of the types of ion species; a_i is Riedel's characteristic constant of the ions for each ion species, and c_i is the concentration (g/L) of the *i-th*ion species. In the present study, seven main components (ion species) were selected for the geothermal fluid samples: Cl^-, Na^+, Ca^+, K^+, SO_4^{-2}, S^+, and Si^+. All the measured data for the three geothermal fluids were fitted to Eq. (2). The derived values of the fitting parameter a_i (Riedel's ion constants) are listed in Table 5. Riedel's model Eq. (2) predicts the measured values of vapor pressure for all the geothermal fluid samples within 3.8%. The values of the ion characteristic constant a_i defined the contribution of each ion species to the total experimentally-observed values of vapor-pressure. This model may be used to predict the vapor-pressure of any geothermal fluid sample with the main components of Cl^-, Na^+, Ca^+, K^+, SO_4^{-2}, S^+, and Si^+, using only pure water data and concentration of the ion species. Riedel [38] used the same correlation model for the thermal conductivity of multi-component aqueous salt solutions, achieving a good prediction agreement (within 5%) with the experimental data for several aqueous salt solutions [39-42, 52-61]. Several authors have examined the accuracy and predictive capability of the Riedel's model (see also, review by Horvath [39]). In the previous publications by our research group [24, 25], the Riedel's

model Eq. (2) was successfully applied for the density, speed of sound, and viscosity correlation for natural geothermal fluids.

Table 5 Values of fitting coefficients (ion species characteristic constants) a_i for Riedel vapor-pressure correlation models Eq. (2) for the main ion species.

Ions	a_i**/ (***l/g***)**
Ca^{+}	-1.2337
K^{+}	0.4047
Na^{+}	-0.0722
S^{+}	-4.2460
Si^{+}	1.5237
Cl^{-}	0.2689
SO_4^{-2}	0.03853
AAD	3.8 %
St. D	5.1 %
Max. D	0.7 %

3.1 Antoine and Wagner-Type Equations for the Vapor-Pressure of Geothermal Fluids

The measured vapor-pressure values of the geothermal fluid samples were used to develop three constant Antoine and multi-parametric Wagner-type [62] correlation equations, for practical applications.

$$\ln P_S = A - \frac{B}{T - C} \tag{3}$$

$$\ln\left(\frac{P_S}{P_{ref}}\right) = \frac{T_{ref}}{T}\left(A\tau + B\tau^{1.5} + C\tau^{3} + D\tau^{3.5} + E\tau^{4} + F\tau^{7.5}\right) \tag{4}$$

Where *A*, *B*, *C*, *D*, *E*, and *F* are the fitting parameters; T_{ref} and P_{ref} are the adjustable reference parameters; and $\tau = 1\text{-}T/T_{ref}$ is the reduced temperature difference. In case of pure liquids (for example, water), T_{ref} and P_{ref} represent the critical temperature and pressure, respectively. Since the critical parameters for geothermal fluids were unknown, T_{ref} and P_{ref} were considered adjustable parameters (or pseudo-critical parameters). The optimal values of the derived parameters in Eqs. (3) and (4) are presented in Table 6 and Table 7. Wagner-type correlation model represented by Eq. (4) has been successfully used previously by several authors to provide vapor-pressure data for a series of pure fluids (see, for example [63]). This equation has also been applied for pure water [62]. The derived values of the pseudo-critical parameters for the geothermal fluids, in the present study, were as follows: Kirchenstollen, T_{ref}=647.2K and P_{ref}= 20,000kPa; Friedrichstollen, T_{ref} = 646.4K and P_{ref} = 20,500kPa; and Murquelle, T_{ref} = 646.4 K and P_{ref}= 20,500kPa. As may be noted, the values of T_{ref} and P_{ref} for the studied geothermal fluid samples are close to those for pure water reported in the results of previous studies [62]. Table 6 and Table 7 also present the deviation statistics between the measured and the calculated values of vapor-pressure for the geothermal fluid samples. The Average Absolute Deviation (AAD) for all the studied samples were within the range of 0.01%–0.03%, consistent with the corresponding experimental uncertainty.

Table 6 Values of fitting coefficients for Antone-type vapor-pressure correlation Eq. (3).

Hot-wells	Kirchenstollen	Friedrichsstollen	Murquelle
A	22.9463	23.1615	23.1685
B	3733.57	3823.20	3817.25
C	43.1965	43.1686	43.0937
AAD (%)	0.01	0.03	0.01
Bias (%)	0.01	-0.03	0.00
St.D (%)	0.01	0.09	0.02
St.Err (%)	0.00	0.02	0.00
Max.D (%)	0.04	0.37	0.05

Table 7 Values of fitting coefficients for Wagner-type vapor-pressure correlation Eq. (4).

Hot-wells	Kirchenstollen	Friedrichsstollen	Murquelle
A	-7.485943	-7.417936	-6.856678
B	1.748927	1.566197	0.399969
C	-12.223745	-14.012622	-15.563151
D	19.985764	21.387856	33.394534
E	-10.986677	-9.846729	-21.746982
F	-3.119380	-5.752147	-1.435095
AAD (%)	0.04	0.04	0.02
Bias (%)	0.05	-0.02	-0.01
St.D (%)	0.10	0.09	0.02
St.Err (%)	0.03	0.02	0.01
Max.D (%)	0.35	0.27	0.07

The derived vapor-pressure correlations (3) and (4) were utilized for the calculation of the other crucial thermodynamic properties of the studied geothermal fluids, such as enthalpy ΔH_{vap} and entropy ΔS_{vap} of vaporization and the isobaric heat capacity ΔC_p, using following thermodynamic relations:

$$\Delta H_{vap} = T\Delta V_S \frac{dP_S}{dT} \quad (5)$$

$$\Delta S_{vap} = \frac{dP_S}{dT}\Delta V_S \quad (6)$$

where ΔH_{vap} and ΔS_{vap} are the enthalpy and entropy of vaporization, respectively; P_S and $\Delta V_S = V'' - V'$ are the vapor pressure and the specific volume changes upon vaporization (vapor and liquid specific volumes at saturation), respectively, caused due to the change of phase; and $\frac{dP_S}{dT}$ is the thermal-pressure coefficient in the saturation curve. Since the volume of vapor is much higher than the volume of liquid ($V'' \gg V'$, $\Delta V_S \approx V'' = RT/P$), then Eqs. (5) and (6) become:

$$\Delta H_{vap} = \frac{RT^2}{P}\frac{dP_S}{dT} \text{ and } \Delta S_{vap} = \frac{RT}{P}\frac{dP_S}{dT} \quad (7)$$

The isobaric heat capacity may be calculated using the following equation:

$$\Delta C_{\mathrm{P}} = 2RT \frac{d \ln P_S}{dT} + RT^2 \frac{d^2 \ln P_S}{dT^2} \quad (8)$$

where vapor-pressure temperature derivative $\frac{dP_S}{dT}$ was calculated using Eqs. (3) and (4). The derived values of the thermodynamic function for all the studied geothermal samples are presented in Table 8 and in Figure 6 and Figure7.

Table 8 Derived thermodynamic properties of the geothermal fluids.

***T* /K**	***P*/kPa**	***ΔH*$_{vap}$ /** kJ·mol^{-1}	***ΔS*$_{vap}$ /** kJ·K^{-1}·mol^{-1}	***ΔC*$_p$ /** kJ·K^{-1}·mol^{-1}
Kirchenstollen				
274.17	0.882	43.737	0.159	6.062
278.16	1.160	43.503	0.156	5.826
282.73	1.571	43.245	0.153	5.573
292.32	2.863	42.738	0.146	5.091
303.16	5.348	42.213	0.139	4.618
313.20	9.123	41.767	0.133	4.235
322.98	14.792	41.365	0.128	3.906
333.16	23.632	40.978	0.123	3.602
343.17	36.315	40.624	0.118	3.337
353.16	54.238	40.295	0.114	3.100
363.10	78.858	39.989	0.110	2.888
373.10	112.328	39.701	0.106	2.696
383.15	156.961	39.430	0.103	2.521
393.18	215.024	39.176	0.100	2.363
403.16	289.029	38.937	0.097	2.220
413.11	*382.021*	*38.713*	*0.094*	*2.091*
Friedrichstollen				
274.17	0.743	44.776	0.163	6.355
278.15	0.984	44.538	0.160	6.109
283.47	1.410	44.232	0.156	5.801
298.76	3.653	43.430	0.145	5.034
308.38	6.284	42.976	0.139	4.627
318.17	10.499	42.549	0.134	4.260
323.32	13.556	42.337	0.131	4.084
333.17	21.549	41.954	0.126	3.777
343.16	33.427	41.592	0.121	3.499
353.15	50.404	41.256	0.117	3.250
363.10	73.970	40.943	0.113	3.028
373.12	106.324	40.647	0.109	2.826
383.11	149.458	40.372	0.105	2.644
393.14	206.284	40.111	0.102	2.479

403.10	279.164	39.868	0.099	2.329
413.13	*372.297*	*39.637*	*0.096*	*2.192*
		Murquelle		
274.18	0.773	44.677	0.163	6.326
278.15	1.021	44.440	0.160	6.082
283.36	1.452	44.142	0.156	5.782
292.20	2.552	43.667	0.149	5.321
301.47	4.423	43.206	0.143	4.893
313.15	8.379	42.673	0.136	4.424
323.19	13.908	42.253	0.131	4.071
333.17	22.228	41.867	0.126	3.761
343.18	34.478	41.506	0.121	3.484
353.19	51.984	41.170	0.117	3.236
363.10	76.107	40.860	0.112	3.016
373.11	109.283	40.566	0.109	2.815
383.13	153.665	40.291	0.105	2.634
393.15	211.895	40.031	0.102	2.469
403.14	286.758	39.788	0.099	2.320
413.13	*381.781*	*39.559*	*0.096*	*2.183*

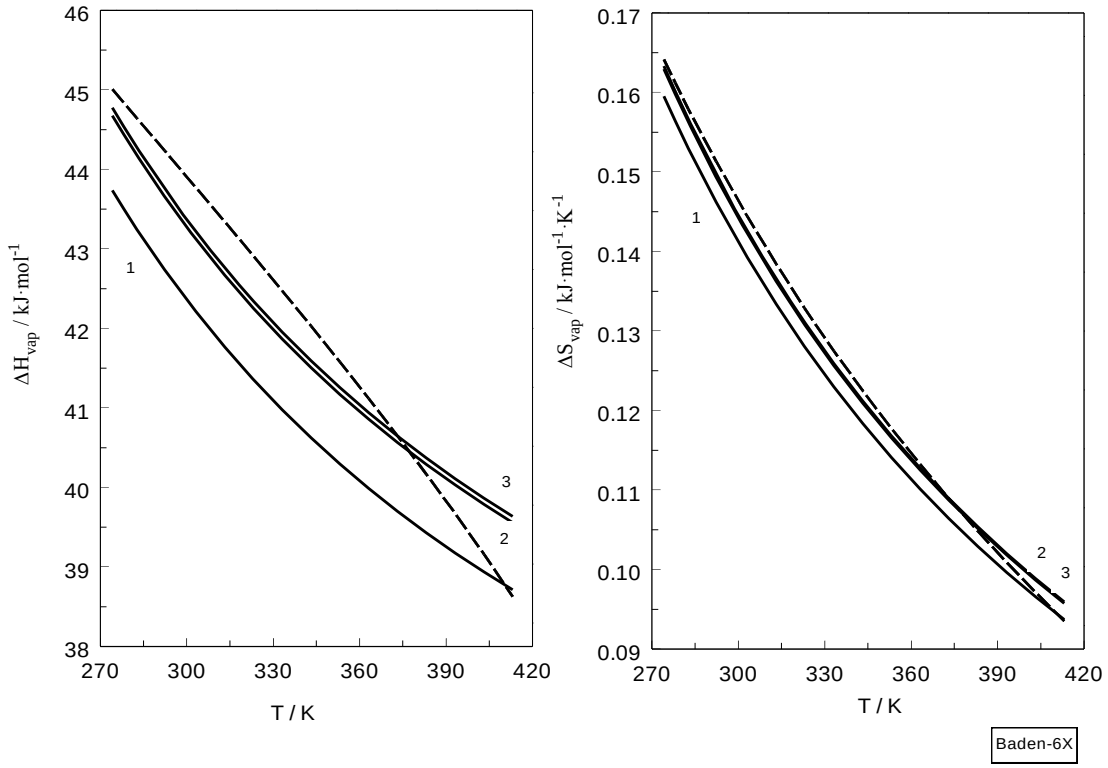

Figure 6 Derived values of enthalpy (left) and entropy (right) of vaporization for geothermal fluids as a function of temperature together with pure water values calculated from IAPWS formulation [48]. 1-Kirchenstollen; 2-Friedrichstollen; and 3-Murquelle; Dashed line is pure water [48].

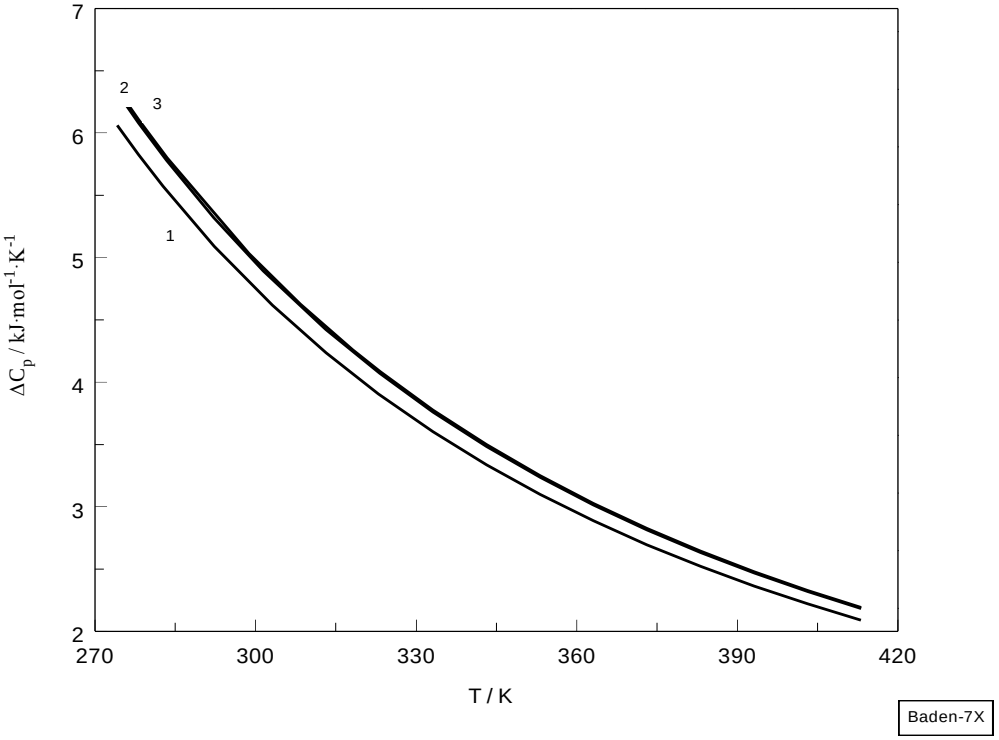

Figure 7 Derived values of heat capacity of geothermal fluids as a function of temperature. 1-Kirchenstollen; 2,3-Friedrichstollen and Murquelle.

4. Conclusions

In the present study, the vapor-pressure of three natural geothermal fluid samples collected from the Baden-Baden geothermal field (Kirchenstollen, Friedrichstollen, and Murquelle, Germany) were measured over the temperature range of 274–413 K using two different methods and vapor-pressure apparatus. The study revealed that the measured vapor-pressures of the geothermal fluids were strongly dependent on the total salt contents (salinity), as well as on the nature of the chemical composition (ion species) and dissolved gases. The measured vapor-pressure values for the geothermal fluids were higher than those of pure water (IAPWS standard data), by a factor of 5.5%–25.4% for the Kirchenstollen sample, 3.0%–11.4% for the Friedrichstollen sample, and 5.3%–14.8% for the Murquelle sample, depending on the measurement temperature. The maximum deviations (in the range of 11%–25%) were observed at low temperatures (approximately 277 K), while at high temperatures, the deviations were within the range of 3.0%–5.5%. This could be attributed to the effect of soluble gases in the geothermal fluids. The soluble gases exerted a strong effect on the measured vapor-pressure of the geothermal fluids. Large differences in the range of 2.6%–18.7% were obtained between the vapor-pressure data for the Kirchenstollen and Friedrichstollen samples, while the data for Kirchenstollen deviated from those of Murquelle by 0.1%–14%. The relatively low difference, ranging from 2.5% to 3.9% was obtained between the Friedrichstollen and Murquelle geothermal fluid samples. It was determined experimentally that different types of ion species exerted different effects on vapor pressure. For instance, Cl^-, SO_4^{-2} and Na^+ ions were observed to exert opposite effects on vapor pressure, i.e., at a constant temperature, Cl^- was observed to be increasing the vapor-pressure, while Na^+ was decreasing it. In general, anions were observed to be increasing, while cations were observed to be decreasing the

vapor-pressure. The rate, $(\partial P_S / \partial c_i)_{T,C_{j\neq i}}$, of these increases or decreases was different and depended strongly on the chemical nature of the ion species. For instance, the same concentrations of Cl^- and Na^+ ions exerted different effects on the measured vapor-pressure; at a temperature of 413 K, the value of the $(\partial P_S / \partial c_i)_{T,C_{j\neq i}}$ for Cl^- was 57.2 kPa/(g/L), while that for Na^+ ions was -350.02 kPa/(g/L). A Riedel-type model for the prediction of vapor-pressures for various concentrations of ion species and temperatures ranging from 274 to 413 K was developed using the measurement data obtained in the experiments. Riedel's characteristic constant of the ions was estimated for each ion species. The contributions of the basic ion species in the geothermal fluids (Na^+, Ca^+, S^+, Si^+, K^+, SO_4^{-2}, and Cl^-) to the total experimentally-observed values of vapor-pressure were also estimated. The measured vapor-pressure data were utilized to develop Antoine and Wagner-type correlation models. Using the measured vapor-pressure data, values of the key derived thermodynamic properties of the geothermal fluid samples (enthalpy and entropy of vaporizations and the heat capacity) were calculated as a function of temperature. The developed models reproduced the measured values of vapor-pressure for the geothermal fluids, with AAD=0.01%–0.03%, St. Dev=0.01%–0.09%, and Max. Dev=0.04%–0.37%.

Author Contributions

Ilmutdin Abdulagatov coordinated and developed the research phases and the manuscript. Misirkhan Talybov performed the measurements of the vapor-pressure for the geothermal fluid samples. Lala Azizova interpreted and evaluated the experimental data, developed vapor-pressure correlation models.

Competing Interests

The authors have declared that no competing interests exist.

References

1. Paschen H, Oertel D, Grünwald R. Möglichkeiten geothermischer Stromerzeugung in Deutschland. Berlin: Büro für Technikfolgen-Abschätzung beim Deutschen Bundestag (TAB); 2003.
2. Kaltschmitt M, Streicher W, Wiese A. Erneuerbare Energien, 4. Aktualisierte und ergänzte Auflage. Berlin: Springer Verlag; 2006.
3. Haas JL. Physical properties of the coexisting phases and thermochemical properties of the H_2O component in boiling NaCl solutions. Washington: Superintendent of Documents, U.S. Government Printing Office; 1976.
4. Sanner B. Baden-Baden a famous thermal spa with a long history. GHC Bull. 2000; 9: 16-22.
5. Vetter C. Geothermal Simulation- GESI, Programmbeschreibung und Validierung. Karlsruher Institut für Technologie Institut für Kern- und Energietechnik, Karlsruher Institut für Technologie; 2014.
6. Vetter C, Wiemer HJ, Kuhn D. Comparison of sub- and supercritical Organic Rankine Cycles for power generation from low-temperature/low-enthalpy geothermal wells, considering specific net power output and efficiency. Appl Ther Eng. 2013; 51: 871-879.

7. Schrüder E, Neumaier K, Nagel F, Vetter C. Study on heat transfer in heat exchangers for a new supercritical organic rankine cycle. Heat Transfer Eng. 2014; 35: 1505-1519.
8. Stefánsson A, Driesner T, Bénézeth P. Thermodynamic of geothermal fluids. Mineralogical Society of America & Geochemical Society; 2012. 76 p.
9. Reindl J, Shen H, Bisiar T. Reservoir engineering: An introduction and application to rico. Colorado, Geothermal Energy-MNGN598; 2009.
10. Schröder E, Thomauske K, Schmalzbauer J, Herberger S, Gebert C, Velevska M. Design and test of a new calorimeter for online detection of geothermal water heat capacity. Geothermics. 2015; 53: 202-212.
11. Herfurth S, Schröder E, Thomauske K, Kuhn D. Messung physikalischer thermalwassereigenschaften unter In-situ- Bedingungen. Essen: Deutscher Geothermiekongress; 2015.
12. Schröder E, Thomauske K, Schmalzbauer J, Herberger S. Measuring techniques for in situ measurements of thermodynamic properties of geothermal water. Melbourne: Proc. World Geothermal Congress 2015; 2015.
13. Birner J. Hydrogeological model of the Malm aquifer in the South German Molasse Basin. Berlin: der Freien Universität Berlin; 2013.
14. Stober I. Auswirkungen der physikalischen Eigenschaften von Tiefenwüssern auf die geothermische Leistung von Geothermieanlagen und die Aquiferparameter. Z GeolWiss. 2013; 41: 9-20.
15. Walsh SDC. Nagasree G, Allan MML, Martin OS. Calculating thermophysical fluid properties during geothermal energy production with NESS and Reaktoro. Geothermics. 2017; 70: 146-154.
16. Bourcier WL, Lin M, Nix G. Recovery of minerals and metals from geothermal fluids, USRL-CONF-215135. OH, United States: 2003 SME Annual Meeting Cincinnati; 2003.
17. Francke H, Thorade M. Density and viscosity of brine: An overview from a process engineers perspective. Chem Erde Geochem. 2010; 70: 23-32.
18. Rogers PSZ, Pitzer KS. Volumetric properties of aqueous sodium chloride solutions. J Phys Chem Ref Data. 1982; 11: 15-81.
19. Zezin D, Driesner T, Sanchez-Valle C. Volumetric properties of mixed electrolyte aqueous solutions at elevated temperatures and pressures. The systems $CaCl_2$-NaCl-H_2O and MgCl-NaCl-H_2O to 523.15, 70 MPa, and ionic strength from (0.1 to 18) mol·kg^{-1}. J Chem Eng Data. 2014; 60: 1181-1192.
20. Anderson G, Probst A, Murray L, Butler S. An accurate PVT model for geothermal fluids as represented by H2O+NaCl+CO_2 mixtures. Stanford: Proc. 17 th Workshop on Geothermal Reservoir Engineering; 1992.
21. McKibbin R, McNabb A. Mathematical modeling the phase boundaries and fluid properties of the system H_2O+NaCl+CO_2. Auckland: Proc. 17th New Zealand Geothermal Workshop; 1995.
22. Millero FJ, Huang F. The density of seawater as a function of salinity (5 to 70 g kg^{-1}) and temperature (273.15 to 363.15 K). Ocean Sci. 2009; 5: 91-100.
23. Ostermann RD, Paranjpe SG, Godbole SP, Kamath VA. The effect of dissolved gas on geothermal brine viscosity. California: Proc 56th Ann Soc Petrol Eng California Regional Meeting; 1986.

24. Abdulagatov IM, Akhmedova-AzizovaL A, Aliev RM, Badavov GB. Measurements of the density, speed of sound, viscosity and derived thermodynamic properties of geothermal fluids. J Chem Eng Data. 2016; 61: 234-246.
25. Abdulagatov IM, Akhmedova-Azizova LA, Aliev RM, Badavov GB, Measurements of the density, speed of sound, viscosity and derived thermodynamic properties of geothermal fluids. Part II. Appl Geochem. 2016; 69: 28-41.
26. Talibov MA, Safarov JT, Hassel ER, Abdulagatov IM. High-pressure and high-temperature density and vapor-pressure measurements and derived thermodynamic properties of natural waters of Yardymli district of Azerbaijan. High Temp High Pres. 2018; 47: 223-255.
27. Abdulagatov IM, Dvoryanchikov VI. Thermodynamic properties of geothermal fluids. Russian J Geochem. 1995; 5: 612-620.
28. Palliser Ch, McKibbin R. A Model for deep geothermal brines, II: Thermodynamic properties-density. Transport Porous Med. 1998; 33: 129-154.
29. Palliser Ch. A model for deep geothermal brines: State space description and thermodynamic properties. Auckland: Massey University; 1998.
30. Dittman GL. Calculation of brine properties, Lawrence Livermore Laboratory, Report UCID 17406; 1977.
31. Potter RW, Haas JL. A model for the calculation of the thermodynamic properties of geothermal fluids. Geoth Resour Council. 1977; 1: 243-244.
32. Dolejs D, Manning CE. Thermodynamic model for mineral solubility in aqueous fluids: theory, calibration and application to model fluid-flow systems. Geofluids. 2010; 10: 20-40.
33. Palliser Ch, McKibbin R. A Model for deep geothermal brines, III: Thermodynamic properties-enthalpy and viscosity. Transport Porous Med. 1998; 33: 155-171.
34. Alkan H, Babadagli T, Satman A. The prediction of the PVT/Phase behavior of the geothermal fluid mixtures. Proceeding of the World Geothermal Congress; 1995. 1659-1665 p.
35. Champel B. Discrepancies in brine density databases at geothermal conditions. Geothermics. 2006; 35: 600-606.
36. Spycher N, Pruess K. A model for thermo physical properties of CO_2-brine mixtures at elevated temperatures and pressures. Stanford: Proc. 36th Workshop on Geothermal Reservoir Engineering; 2011.
37. Wahl EF. Geothermal energy utilization. New York: Wiley; 1977.
38. Riedel L. The heat conductivity of aqueous solutions of strong electrolytes. Chem Ing Tech. 1951; 23: 59-64.
39. Horvath AL. Handbook of aqueous electrolyte solutions. Ellis Horwood: Physical Properties, Estimation Methods and Correlation Methods; 1985.
40. Aseyev GG, Zaytsev ID. Estimation methods and experimental data. New-York: Begell-House; 1996.
41. Aseyev GG. Methods for calculation of the multicomponent systems and experimental data on thermal conductivity and surface tension. New York: Begell-House; 1998.
42. Abdulagatov IM, Assael M. Viscosity. Hydrothermal properties of materials. London: John Wiley & Sons; 2009. 249-270 p.
43. Agemar T, Alten JA, Ganz B, Kuder J, Kьhne K, Schumacher S, et al. The geothermal information system for Germany-GeotIS. Z Dtsch Ges Geowiss. 2014; 165: 129-144.

44. Suchi E, Dittmann J, Knopf S, Müller C, Schulz R. Geothermal Atlas to visualize potential conflicts of interest between CO_2 storage (CCS) and deep geothermal energy in Germany. Z Dtsch Ges Geowiss; 2014.
45. Ganz B, Schellschmidt R, Schulz R, Sanner B. Geothermal energy use in Germany. Pisa, Italy: European Geothermal Congress; 2013.
46. Helgeson HC. Solution chemistry and metamorphism. Res Geochem. 1967; 55: 379-385.
47. Lemmon EW, Bell IH, Huber ML, Mc Linden MO. NIST Standard Reference Database 23, NIST Reference Fluid Thermodynamic and Transport Properties, REFPROP, version 10.0, Standard Reference Data Program, National Institute of Standards and Technology: Gaithersburg, MD; 2018.
48. Wagner W, Pruß A. New international formulation for the thermodynamic properties of ordinary water substance for general and scientific use. J Phys Chem Ref Data. 2002; 31: 387-535.
49. Haar L, Gallagher TS, Kell GS. NBS/NRS steam tables: Thermodynamic and transport properties and computer programs for vapor and liquid states in SI units. Washington: Hemisphere; 1984. 120 p.
50. Fabuss BM, Korosi A. Vapor pressures of binary aqueous solutions of NaCl, KCl, Na2SO4, and MgSO4 at concentrations and temperatures of interest in desalination processes. Desalination. 1966; 1: 139-148.
51. Nie N, Zheng D, Dong L, Li Y. Thermodynamic properties of the water + 1-(2-Hydroxylethyl)- 3-methylimidazolium chloride system. J Chem Eng Data. 2012; 57: 3598-3603.
52. AbdulagatovI M, Magomedov UM. Thermal conductivity of aqueous $ZnCl_2$solutions at high temperatures and high pressures. Ind Eng Chem Res. 1998; 37: 4883-4888.
53. Abdulagatov IM, Akhmedova-Azizova LA, Azizov ND. Thermal conductivity of binary aqueous NaBr and KBr and ternary H_2O+NaBr+KBr solutions at temperatures from 294 to 577 K and pressures up to 40 MPa. J Chem Eng Data. 2004; 49: 1727-1737.
54. Abdulagatov IM, Akhmedova-Azizova LA. Thermal conductivity of aqueous $CaCl_2$ solutions at high temperatures and high pressures. J Sol Chemistry. 2014; 43: 421-444.
55. Abdulagatov IM, Azizov ND, Zeinalova AB. Density, apparent and partial molar volumes, and viscosity of aqueous Na_2CO_3 solutions at high temperatures and high pressures. Z Phys Chem. 2007; 221: 963-1000.
56. Abdulagatov IM, Azizov ND. *PVTx* Measurements and partial molar volumes for aqueous li_2so_4 solutions at temperatures from 297 to 573 k and pressures up to 40 MPa. Int J Thermophys. 2003; 24: 1581-1610.
57. Abdulagatov IM, Azizov ND. Thermal conductivity and viscosity of the aqueous K_2SO_4 solutions at temperatures from 298 to 573 K and at pressures up to 30 MPa. Int J Thermophys. 2005; 26: 593-635.
58. Abdulagatov IM, Azizov ND. Viscosity of aqueous $CaCl_2$solutions at high temperatures and high pressures. Fluid Phase Equilib. 2006; 240: 204-219.
59. Abdulagatov IM, Azizov ND. Densities, apparent and partial molar volumes of concentrated aqueous LiCl solutions at high temperatures and high pressures. Chem Geology. 2006; 230: 22-41.

60. Abdulagatov IM, Zeinalova AB, Azizov ND. Viscosity of aqueous Na_2SO_4 solutions at temperatures from 298 to 573 K and at pressures up to 40 MPa. Fluid Phase Equilib. 2005; 227: 57-70.
61. Abdulagatov IM, Azizov ND, Zeinalova AB. Viscosities, densities, apparent and partial molar volumes of concentrated aqueous $MgSO_4$ solutions at high temperatures and high pressures. Phys Chem Liq. 2007; 45: 127-148.
62. Wagner W, Saul A. Proc 10th International Conference on the Properties of Steam. Moscow: Mir; 1986. 199 p.
63. Lemmon EW, Goodwin ARH. Critical Properties and Vapor Pressure Equation for Alkanes C_nH_{2n+2}: Normal Alkanes with n <= 36 and Isomers for n = 4 Through n = 9. J Phys Chem Ref Data. 2000; 29: 1-39.